ORIGINAL PAPER

The investigation of treatment design parameters on carbon integration networks

Sabla Y. Alnouri[1] · Dhabia M. Al-Mohannadi[2]

Abstract

Carbon Integration methods help identify the appropriate allocation of captured carbon dioxide (CO_2) streams into CO_2-using sinks, and are especially useful when a number of CO_2 sink options are present simultaneously. The method helps identify CO_2 allocation scenarios when subjected to an emission target on the CO_2 overall network. Many carbon dioxide sink options are costly, and more often than not, require a high purity carbon dioxide source to satisfy the sink demand. Hence, it is imperative to effectively incorporate treatment units in such networks, to obtain high-purity CO_2 streams. In fact, it has been previously reported in many studies that the most expensive step in Carbon Capture, Utilization and Sequestration (CCUS) is the treatment system. As a result, this paper focuses on reassessing the performance of carbon integration networks using a more rigorous cost model for the treatment design stage. The effect of utilizing different treatment operating conditions on the overall cost of the treatment stage of CO_2 (before allocation) is first captured using a detailed cost model. Subsequently, this information is then fed into a network design problem that involves a CO_2 source-sink allocation network problem, and different CO_2 net capture targets within the network. For this, an enhanced treatment model that captures all necessary treatment design parameters has been utilized alongside the original model. The original carbon integration formulation has been adopted from previous work. Many of the cost items have been lumped into single parameters in the original formulation, and lack the necessary depth required to carry out the necessary investigations for this work. Hence, the treatment model introduced in this paper is more rigorous, as it accounts for important technical performance constraints on the system to be assessed. Utilizing a more detailed cost model was found to be very helpful in understanding several effects of varying parameters on the overall source-sink allocations, when subjected to different CO_2 net emission reduction targets. The cost of the carbon network increases when the solvent temperatures are increased. However, there was a noticeable linear trend at lower temperatures compared to higher temperatures, where the increase became non-linear. Furthermore, it was discovered that for net capture targets of 20% and 25%, no revenue from carbon storage could be generated beyond a solvent temperature of 25 °C. Additionally, the optimal diameter of the treatment column was more responsive to changes in solvent temperature for cases with low net capture targets (below 10%), while its sensitivity decreased for higher capture targets (above 10%).

Keywords Carbon integration · GHG emissions · Treatment · Carbon dioxide · Cost model

List of symbols

C^{Col}	Column vessel cost ($)
C^{Pack}	Packing cost ($)
C^{Op}	Operating cost ($)
γ	Plant lifetime (years)
C^{V}	Packing cost per unit volume ($/m^3)
Q_G	Volumetric flowrate of the gaseous stream (m^3/h)
v_G	Gas velocity (m/s)
v_G^{flood}	Gas velocity at flooding conditions (m/s)
f^{flood}	Flooding factor
C_S^{flood}	Coefficient at flooding conditions
ρ_G	Density of the gaseous stream (kg/m^3)
ρ_L	Density of the liquid stream (kg/m^3)
a_1	Equation parameter
a_2	Equation parameter
a_3	Equation parameter
b_1	Equation parameter
b_2	Equation parameter

✉ Dhabia M. Al-Mohannadi
dhabia.al-mohannadi@qatar.tamu.edu

1 Gas Processing Centre, College of Engineering, Qatar University, PO Box 2713, Doha, Qatar

2 Chemical Engineering Department, Texas A&M University at Qatar, PO Box 23874, Doha, Qatar

b_3	Equation parameter
T	Temperature (K)
Y^{flood}	Pressure drop parameter at flooding conditions
X	Flow parameter
$m_{L(1)}$	Amount of solvent liquid exiting the column (kg/h)
$m_{L(1)}$	Amount of solvent liquid exiting the column (kg/h)
$m_{CO_2(abs)}$	Amount of CO2 absorbed (kg/h)
$y_{CO_2(1)}$	Mole fraction of CO_2 in the gaseous stream entering the column
M_G	Molecular weight of the gaseous stream
%R	Percentage removal of carbon dioxide
M_{CO_2}	Molecular weight of carbon dioxide (kg/koml)
M_{air}	Molecular weight of air (kg/koml)
$y_{air(1)}$	Mole fraction of air in the gaseous stream entering the column
F_P	Packing factor
μ_L	Viscosity of the liquid stream (mPa s)
D	Column Dimeter (m)
h	Packing Height (m)
F^{mat}	Material Factor
P	Operating pressure kPa
H_{OG}	Overall height of a gas-phase transfer unit (HTU)
N_{OG}	Overall number of gas-phase transfer units (NTU)
G	Molar flowrate of the gaseous stream (kmol/h)
$K_y a$	Overall mass transfer coefficient (kmol/s m^2)
A_c	Cross sectional area of the column (m^2)
m	Slope of the operating line
H	Henry's constant for CO_2 in the solvent (atm m^3/kmol)
c_s	Concentration of the solvent (kmol/m^3)
x_A	Initial concentration of CO_2 in the solvent
S	Molar flowrate of the solvent entering the column (kmol/s)

Introduction

Carbon capture, utilization and sequestration (CCUS) refers to technologies that can capture and make use of carbon dioxide (CO_2) emitted by industrial activities. Process emissions from cement, iron and steel, and chemical production are among the most challenging to abate (IEA 2019). Hence, CCUS plays a key role in decarbonization, having emerged as one of the most promising solutions to the global climate change. It should be noted that both utilization 'U' and storage 'S' play very important roles in reducing greenhouse gas (GHG) emissions. CO_2 utilization generally involves the conversion of CO_2 into valuable products (Zhang et al. 2020). Hence, CO_2 may be used as feedstock for the production of various chemicals, fuels, and materials. For example, CO_2 can be converted into methanol, which can be used as a fuel or a chemical building block. Additionally, CO_2 can be utilized in the production of polymers, plastics, concrete, and other chemicals (Madejski et al. 2022). CO_2 can also be reacted with minerals, such as calcium or magnesium silicates, to produce stable carbonates (Zhang et al. 2020). Hence, utilizing CO_2 instead of releasing it into the atmosphere can potentially create a carbon–neutral or carbon-negative cycle (Al-Mamoori et al. 2017). On the other hand, CO_2 storage refers to the process of capturing CO_2 emissions and permanently storing them, so as to prevent their release into the atmosphere. There exist many different methods for carbon storage such as (1) geological storage, which involves injecting the CO_2 deep underground into geological formations (Fagorite et al. 2023); (2) ocean storage which involves injecting the CO_2 deep in the ocean (Goldthorpe 2017); and (3) biological storage, which involves storing CO_2 using forests, wetlands, and other similarly functioning ecosystems that can naturally sequester carbon dioxide by absorbing it from the atmosphere then incorporating it into plant biomass and soil organic matter (Guduru et al. 2022). By combining efficient utilization and storage strategies, CO_2 emissions can be reduced effectively. Utilization focuses on minimizing emissions at the source and transitioning to cleaner alternatives, while storage helps offset and capture the remaining emissions that are challenging to eliminate completely. This comprehensive approach plays a crucial role in combating climate change, via the mitigation of GHG and CO_2 emissions (Centi and Perathoner 2023).

CCUS typically involves several steps starting from the capture of CO_2 from emission sources, followed by the transportation of CO_2 to their final destinations, which in turn may take the form of geological sequestration, or the utilization of CO_2 in appropriate conversion processes such as methanol (Xu et al. 2005). Some CCUS steps may be more challenging than others, due to their large energy requirements (Najjar 2008). For instance, one of the major CCUS cost influencers is the need for an energy-intensive CO_2 treatment unit. Treatment becomes especially expensive if very dilute CO_2 streams are involved (IPCC 2005). In fact, carbon dioxide treatment process incurs substantial expenses within the carbon capture utilization and storage supply chain. The costs of energy and capital linked to CO_2 treatment play a crucial role in the development of effective and financially feasible carbon capture solutions. This research aims to tackle this obstacle by examining the ideal treatment conditions that can enhance the economic viability and efficiency of carbon network design.

There has been a plethora of work in the area of carbon capture using adsorption, absorption, and membrane processes (Ochedi and Taki 2022) each varying in efficiency

and cost. Absorption in an aqueous amine solution is currently the most mature industrial process that can be used to capture anthropogenic CO_2 (de Meyer and Bignaud 2022). Beyond CCUS, most of the industrial acid gas removal (AGR) units employ chemical absorption process for the removal of acid gases from natural gas, with diglycolamine (DGA) and monoethanol amine (MDEA) being reported as the most widely used to achieve acceptable sweet gas purities (Zahid 2020). With regards to the use of ionic liquid alternatives. Hospital-Benito et al. (2021) evaluated ionic liquids based on CO_2 chemical capture processes and costs. Budinis et al. (2018) reported costs that vary from 20 to 110 USD per ton of CO_2. Luis (2016) gives overview of the main implications of using MEA as absorption solvent for CO_2 capture together with the last advances in research to improve the conventional absorption process. Li et al. (2016) investigated the technical and economic performance of the monoethanolamine (MEA)-based post-combustion capture process and its improvements integrated with a 650-MW coalfired power station. Zhang et al. (2019) examined different mechanisms that trigger phase separations in solvents including those subjects to chemically or thermally triggered phase changes, non-aqueous or aqueous systems, and those forming either a CO_2-enriched solid or a liquid phase are provided and their physiochemical properties in CO_2 capture. Gonzalez et al. (2023) developed a process model for H_2S and CO_2 absorption with a blended solvent, which is based on new thermodynamic, kinetic, and physical experimental data. The main idea was to lower the high energy demand for the regeneration process by using a physical co-solvent

with a lower specific heat. Hussin and Aroua reported many of the recently published articles and patents on CO_2 capture technologies via adsorption from 2014 to 2018. Various types of adsorbents that can be potentially used to capture CO_2 have been discussed in their work (Hussin and Aroua 2020).

Having observed many of the present work in literature, currently, the most cost efficient and widely applied CO_2 separation technology in industry is the CO_2 absorption process. However, the relatively high treatment costs associated with such processes typically prevent its massive deployment (de Meyer and Bignaud 2022). Since many operating parameters may affect the cost of those units, this work aims to understand the effect of varying the operating conditions within the treatment stage of the network (which consists of a CO_2 absorption unit), on the cost of a CO_2 integration network. Many of the CCUS cost models that have been utilized in previous studies involve a single lumped cost estimation parameter to represent the treatment unit, without any considerations of the detailed design of those units. Figure 1 illustrates the various components of a CO_2 integration network. The mathematical formulation associated with a CO_2 integration problem has been previously developed and presented by Al-Mohannadi and Linke (2016). In this work, the treatment unit model has been revisited, and a detailed cost model for the treatment stage within the source-sink allocation network problem has been used to investigate the effect of varying the operating conditions of the treatment stage onto the overall CO_2 network cost and performance. An appropriate treatment model has been developed integrated onto
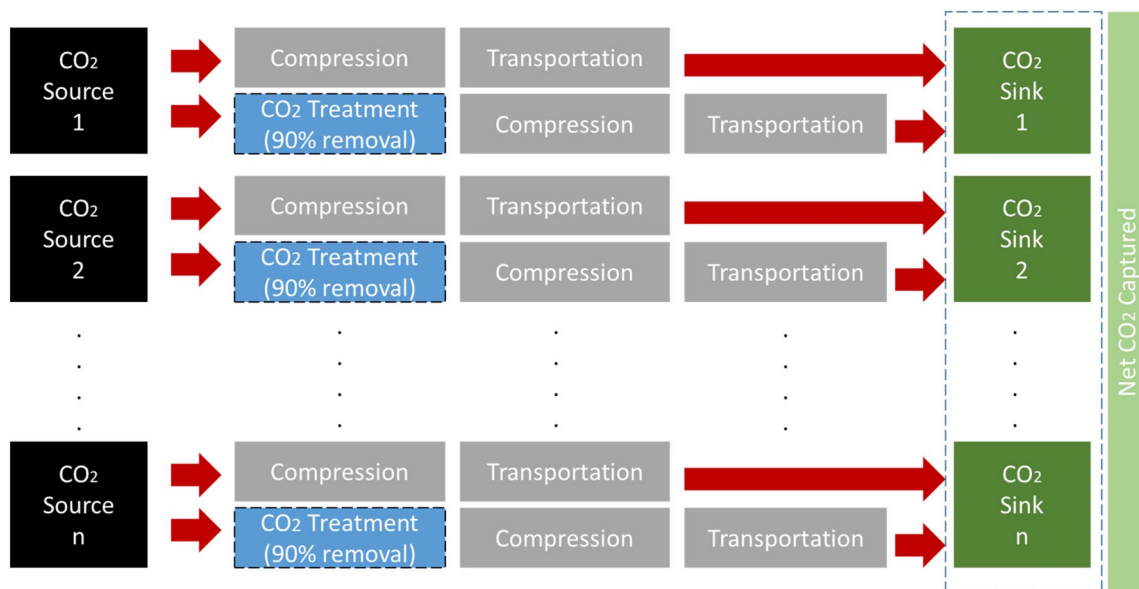

Fig. 1 Illustration of the various components of a carbon integration network

the original CO_2 Integration model which in turn has been adopted from (Al-Mohannadi et al. 2015; Al-Mohannadi and Linke 2016).

Currently, existing carbon integration models incorporate a simplified model for the treatment stage (Al-Mohannadi et al. 2015; Al-Mohannadi and Linke 2016). Incorporating a more detailed treatment model into carbon integration investigations can capture the intricacies and complexities of CO_2 treatment within the overall CO_2 network, and hence provide a more realistic representation of the system. Moreover, a deeper understanding of the carbon integration network performance can be obtained, by obtaining insights into the various factors and variables that affect the system's performance, enabling a comprehensive analysis of the process. This understanding is crucial for optimizing and fine-tuning the CO_2 network, as well as maximize its efficiency and effectiveness. Moreover, incorporating more details into the treatment model for carbon integration problems helps explore different scenarios, configurations, and operating conditions within the treatment unit, as well as evaluate the impact of various parameters (such as temperature, type of solvent etc..) so as to identify optimal network conditions that can lead to improved carbon integration performance.

Mathematical model

The following section details all the necessary modifications that have been implemented onto the treatment design cost model, which were found to also involve other key performance parameters. The treatment model below is able to quantify the following three different solvent properties (density, viscosity, and Henry's constant) onto the cost of the treatment stage within the CCUS network.

The cost of the column has been found using Eq. (1) below:

$$C^{Col} = 682.8(D)^{0.675} h F^{mat} \left(\frac{14.5P}{50} \right)^{0.44} \tag{1}$$

where C^{Col} is the column cost, D is the diameter of the column, h is the packing height, F^{mat} is a material factor, and P is the operating pressure of the column. A number of

material factors obtained Brunazzi et al. (2002) are provided in Table 1.

The cost of the packing of the column has been found using Eq. (2) below:

$$C^{Pack} = \frac{\pi(D)^2}{4} h C^V \tag{2}$$

where C^{Pack} is the column cost, D is the diameter of the column, h is the packing height, and C^V is the packing cost per unit volume. A number of packing volumes also obtained from Brunazzi et al. (2002) are provided in Table 2

The diameter of the column can be calculated using Eq. (3) below:

$$D = \left[\frac{4\left(\frac{Q_G}{3600} \right)}{v_G \pi} \right]^{0.5} \tag{3}$$

where Q_G is the volumetric flowrate of the gaseous stream, and v_G is the gas velocity.

The gas velocity may be computed from the gas velocity at flooding conditions according to Eq. (4) below:

$$v_G = v_G^{flood} f^{flood} \tag{4}$$

where v_G^{flood} is the gas velocity at flooding conditions, and f^{flood} is the flooding factor.

To find the gas velocity at flooding conditions, Eq. (5) below can be used:

$$v_G^{flood} = \frac{C_S^{flood}}{\left[\frac{\rho_G}{\rho_L - \rho_G} \right]^{0.5}} \tag{5}$$

where C_S^{flood} is the coefficient at flooding conditions, and ρ_G is the density of the gaseous stream, while ρ_L is the density of the liquid (solvent).

The liquid (solvent) density ρ_L was found using Eq. (6) below:

$$\rho_L = a_1 + a_2(T) + a_3(T)^2 \tag{6}$$

where a_1, a_2 and a_3 are equation parameters can be obtained from DiGuilio et al. (1992) for various different amine solvents, and T is the temperature of the solvent.

Table 1 Values for the material factor (F^{mat}) of the column (Brunazzi et al. 2002)

Carbon Steel	Stainless 304	Nickel 200
1	1.7	5.4

Table 2 Values for Packing costs per unit Volume (C^v), for a number of different Packing types and materials (Brunazzi et al. 2002)

Structured Packing (AIS316)	Structured Packing (Polypropylene)	Raschig Ring (AIS316)	Raschig Ring (Polypropylene)
2778.75	3926.52	1510.47	241.02

To find the gas velocity at flooding conditions, Eq. (7) below can be used:

$$C_S^{flood} = \left[\frac{Y^{flood}}{F_p \mu_L^{0.1}}\right]^{0.5} \tag{7}$$

where Y^{flood} is the pressure drop parameter at flooding conditions, and F_P is the packing factor, while μ_L is the viscosity of the liquid (solvent).

The liquid (solvent) viscosity μ_L was found using Eq. (8) below:

$$\ln\mu_L = b_1 + \frac{b_2}{T(K) - b_3} \tag{8}$$

where b_1, b_2 and b_3 are equation parameters can be obtained from DiGuilio et al. (1992) for various different amine solvents, and T is the temperature of the solvent.

The pressure drop parameter at flooding conditions Y^{flood} can be obtained using Eq. (9) below:

$$\ln\left[Y^{flood}\right] = -3.5021 - 1.028(lnX) - 0.11093(lnX)^2 \tag{9}$$

where X is the flow parameter, and can be found using Eq. (10) below:

$$X = \frac{m_{L(1)}}{Q_G \rho_G} \left(\frac{\rho_G}{\rho_L}\right)^{0.5} \tag{10}$$

where $m_{L(1)}$ is the mass flowrate of the solvent liquid exiting the column, which in turn can be found using Eq. (11) below:

$$m_{L(1)} = m_{L(2)} + m_{CO_2(abs)} \tag{11}$$

In Eq. (11) above, $m_{L(2)}$ is the mass flow of the solvent liquid entering the column (or the initial solvent flowrate), and $m_{CO_2(abs)}$ is the amount of CO_2 absorbed in the column. To find the latter flowrate, Eq. (12) can be used:

$$m_{CO_2(abs)} = \frac{Q_G \rho_G}{M_G} y_{CO_2(1)}(\%R)(M_{CO_2}) \tag{12}$$

where $y_{CO_2(1)}$ is the mole fraction of CO_2 in the gaseous stream entering the column, M_G is the molecular weight of the gaseous stream, $\%R$ is the percentage removal of carbon dioxide, and M_{CO_2} is the molecular weight of carbon dioxide.

To find the molecular weight of the gaseous stream Eq. (13) can be used:

$$M_G = y_{CO_2(1)}M_{CO_2} + y_{air(1)}M_{air} \tag{13}$$

where M_{air} is the molecular weight of air, and $y_{air(1)}$ is the mole fraction of air in the gaseous stream entering the column.

To find the packing height, Eq. (14) below has been used:

$$h = H_{OG}N_{OG} \tag{14}$$

where H_{OG} represents the overall height of a gas-phase transfer unit (HTU), and N_{OG} represents the overall number of gas-phase transfer units (NTU).

To find the overall height of a gas-phase transfer unit H_{OG}, Eq. (15) has been used:

$$H_{OG} = \frac{G}{K_y a A_c} \tag{15}$$

where G is the molar flowrate of the gaseous stream, $K_y a$ is the overall mass transfer coefficient, while A_c is the cross-sectional area of the column.

The molar flowrate of the gaseous stream is simply the Q_G is the volumetric flowrate of the gaseous stream divided by the density ρ_G, divided by the molecular weight of the gaseous stream M_G.

The cross-sectional area of the column can be found using the column diameter:

$$A_c = \frac{\pi D^2}{4} \tag{16}$$

The overall mass transfer coefficient $K_y a$ can be found using the film coefficients for the flow in the tower $k_x a$ and $k_y a$ according to Eq. (17) below:

$$K_y a = \frac{1}{\frac{1}{k_x a} + \frac{m}{k_y a}} \tag{17}$$

where m is the slope of the operating line, found according to Eq. (18) below:

$$m = \frac{H x_A}{P} \tag{18}$$

where H is Henry's constant for CO_2 in the solvent, x_A is the initial concentration of CO_2 in the solvent, and P is the operating pressure.

To find Henry's constant, Eq. (19) has been used:

$$lnH = c_1 + c_2(T) + c_3(T)^2 \tag{19}$$

where c_1, c_2 and c_3 are equation parameters, and T is the temperature of the solvent.

$$c_1 = d_1 - d_2\left(\frac{C_s}{\rho_L}\right) + d_3\left(\frac{C_s}{\rho_L}\right)^2 + d_4\left(\frac{C_s}{\rho_L}\right)^3 \tag{20}$$

$$c_1 = e_1 - e_2\left(\frac{C_s}{\rho_L}\right) + e_3\left(\frac{C_s}{\rho_L}\right)^2 + e_4\left(\frac{C_s}{\rho_L}\right)^3 \tag{21}$$

$$c_1 = f_1 - f_2\left(\frac{C_s}{\rho_L}\right) + f_3\left(\frac{C_s}{\rho_L}\right)^2 + f_4\left(\frac{C_s}{\rho_L}\right)^3 \tag{22}$$

where d_1, d_2 and d_3, e_1, e_2 and e_3, f_1, f_2 and f_3 are all equation parameters, and c_s is the concentration of solvent.

To find the overall number of gas-phase transfer units N_{OG}, Eq. (23) has been used:

$$N_{OG} = \frac{1}{1 - \frac{mG}{S}} \ln\left[\left(1 - \frac{mG}{S}\right)\frac{y_{in} - y*_{out}}{y_{out} - y*_{out}} + \frac{mG}{S}\right] \tag{23}$$

where G is the molar flowrate of air entering the column, S is the molar flowrate of the solvent entering the column, y_{in} is the concentration of CO_2 in the gaseous stream entering the column, y_{out} is the concentration of CO_2 in the gaseous stream leaving the column, $y*_{out}$ is the equilibrium concentration of CO_2 in the gaseous stream leaving the column.

The molar flowrate of the solvent S is simply the mass flowrate of the solvent $m_{L(2)}$ entering the column divided by the molecular weight of the liquid stream ρ_L

The equilibrium concentration of CO_2 in the gaseous stream leaving the column, $y*_{out}$ can be found from Eq. (20) below:

$$y*_{out} = mx_{in} \tag{24}$$

Based on all of the above, the total cost of the column can be found using Eq. (21) below:

$$C^{Treatment} = \left(C^{Col} + C^{Pack}\right)\gamma + C^{Op} \tag{25}$$

where γ is the plant lifetime, and C^{Op} is the operating cost of the column. The Carbon Integration model outlined by Eqs. (1)–(28) which has been previously introduced by Al-Mohannadi and Linke (2016) has been modified in this work, by replacing the treatment unit costing equation from

the flow of carbon dioxide multiplied by capital cost parameter in the original model, with the new detailed Eq. (21). Moreover, Eqs. (1)–(20) that have been outlined in this section, were all utilized alongside Eq. (21). Moreover, all units of measure that are associated with Eqs. (1)–(21) are provided in the nomenclature section.

The focus of this study was to test the sensitivity of carbon integration networks to changes in the operating conditions within the treatment stage of the design, when subjected to different net capture targets. The model assumptions that are associated with the carbon integration model are summarized in Table 3. It should be noted that the net capture target refers to the equivalent to the amount of CO_2 utilized within the sinks that are available in the network, against the amount emitted. Any unutilized CO_2 is considered to be emitted to the atmosphere. The following section summarizes the illustrative case study that was carried out in this paper.

Case study illustration

The same case study which has been previously introduced by Al-Mohannadi and Linke (2016) has been revised. The case study involves 4 different process sources coming from an Ammonia plant, a Steel-Iron plant, a Power plant and a Refinery. All case study information pertaining to the CO_2 sources and sinks has been adopted from Al-Mohannadi and Linke (2016). Moreover, the CO_2 removal efficiencies has been set to 90% in all treatment units, so as to be able to meet the sink quality requirements. Since each CO_2 stream is considered to be present in a separate plant, a decentralized model for the treatment process has been assumed in this work. Hence, each plant is assumed to carry out its CO_2

Table 3 Carbon Integration model assumptions

#	Assumption
1	An industrial park consists of multiple industrial plants that are already built
2	Plants in the industrial park have processes that emit carbon dioxide from stationary points at fixed steady state flow
3	The emitted carbon dioxide streams are referred to as sources
4	Sources vary in composition, flow rates, and conditions, including purged process streams, flue gases, and other carbon dioxide emitting streams from the plants
5	Processes that receive carbon dioxide-containing feeds are referred to as sinks
6	Sinks can be existing processes in the industrial park or sequestration processes within or outside the park boundaries. They receive, consume, convert, transform, or store carbon dioxide
7	Sinks typically require carbon dioxide with specific purity and pressure levels
8	Separation and compression units may be necessary to prepare source streams according to sink requirements
9	The phase of carbon dioxide delivered is determined by the pressure requirements of the sink
10	For storage and pipeline transportation, carbon dioxide must be compressed to at least 15 MPa
11	The utilization of carbon dioxide in a sink can be a profitable or unprofitable process, and the potential financial gains or losses must be considered in designing the carbon integration network

Table 4 Gas Stream properties

	Gas Stream Flowrate (m³/h)	CO₂ mole fraction in Gas Stream	Density. kg/m³
Ammonia	16,869	1	1.85
Steel-Iron	11,6231	0.44	0.97
Power	52,8435	0.07	0.74
Refinery	56,173	0.27	0.81

treatment process separately. The respective volumetric flowrates Q_G for each of the gaseous streams which have been considered as process sources are provided in Table 4. Moreover, several other properties for each of the streams considered are also provided, such as the initial concentration CO_2 in the gas stream (before treatment), in addition to the density of each of those gaseous streams. It should be noted that the stream coming from the ammonia plant is a pure carbon dioxide stream (hence does not require any treatment prior to utilization). All associated
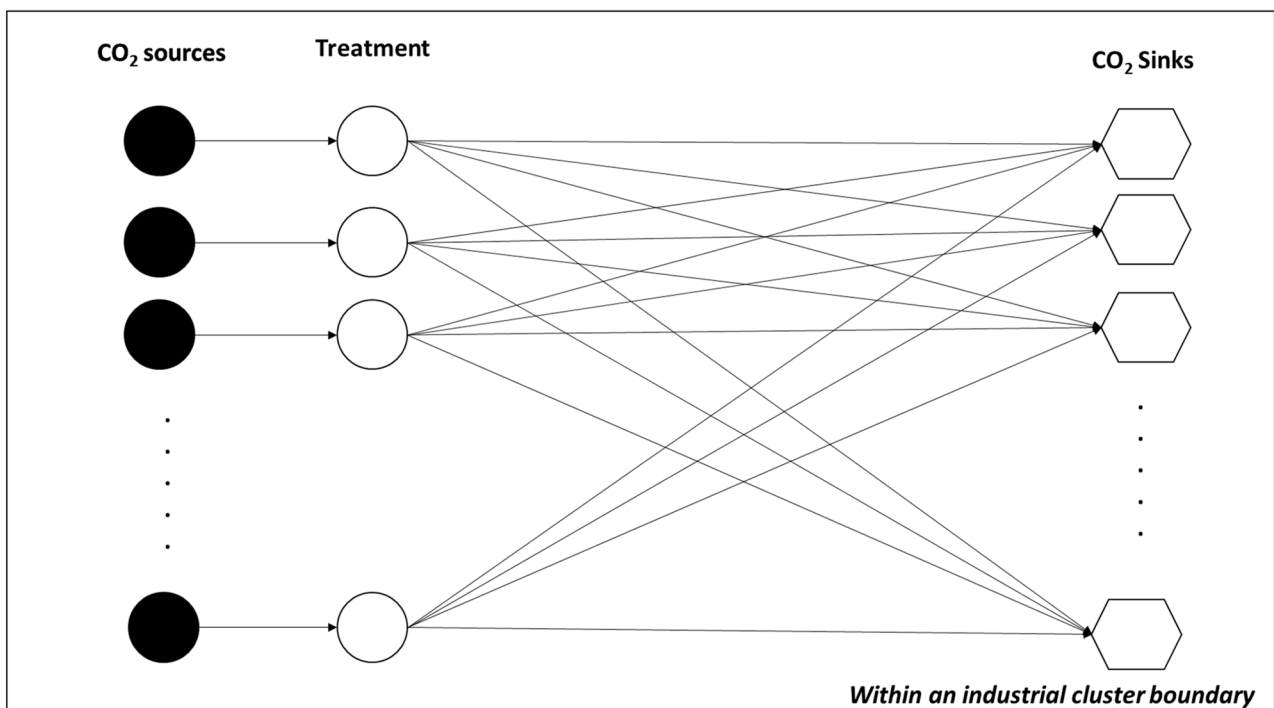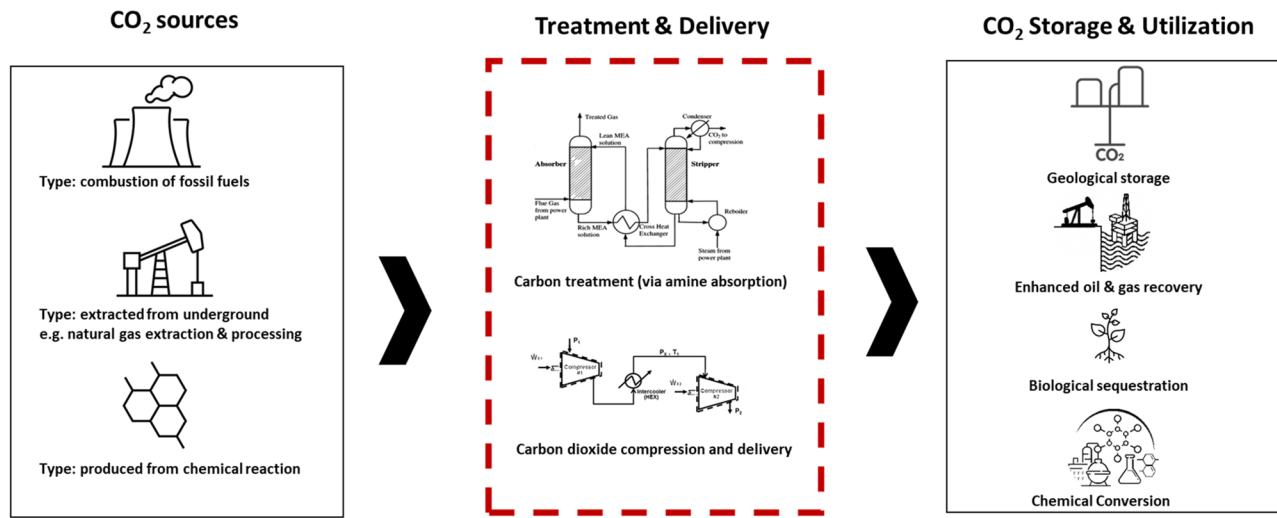
Fig. 2 System Illustration

data for the costing of the compression stations and the pipelines has all been obtained from Al-Mohannadi and Linke (2016). Figure 2 provides an illustration for the evaluated system. All mass balances on the sources and sinks have been carried out according to the mathematical formulation provided by Al-Mohannadi and Linke (2016). In this work, the treatment unit in the original model has been replaced with Eqs. (1)–(21) shown above.

The solvent considered in this work is Methyl diethanolamine (also known as N-methyl-diethanolamine), a very effective for the removal of carbon dioxide from various gaseous streams in the petrochemical industry. Based on this the required properties to be utilized in the treatment model have been obtained from MDEA, and are summarized in Table 5

As such, and after obtaining all the necessary information in terms of the required solvent parameters needed for the (Non-Linear Program) NLP presented above, the effect of varying the solvent temperature over a 10-degree temperature range (20 °C–30 °C) for six different CO_2 capture targets have been made, hence a total of 60 different runs have been carried out. The respective results obtained are summarized in the following section. The optimization problem for each of the cases which have been tested has been carried out using What's Best 9.0.5.0 LINDO Global Solver for Microsoft Excel 2010, has been used to implement the model, on a laptop with Intel® Core™ i7-2620 M, 2.7 GHz, 8.00 GB RAM, 64-bit Operating System (LINDO® 2023). Solving NLPs can be difficult, and achieving convergence to the global optimum is not assured. To enhance convergence and solution quality, it is advisable to possess a comprehensive comprehension of the underlying problem structure and employ suitable solver techniques. In this research, a multi-start solver was employed, enabling multiple optimization runs from distinct initial points. This strategy effectively addresses the difficulty of discovering a globally optimal solution in NLPs, as the initial points encompass a wide range of feasible solutions. It should be noted that all runs managed to converge in less than 780s of CPU time.

Results and discussion

The treatment cost variation obtained as a function of solvent temperature, for different CO_2 net capture targets is summarized in Fig. 3. According to Fig. 3, the treatment cost variation exhibits a linear trend across all temperatures, and net capture targets investigated. Moreover, a major difference was noted when comparing the increase in the treatment cost attained at lower capture cases versus the higher capture cases. For instance, the 5% capture case, which was the lowest capture case considered in this study, exhibited a linear increase in cost across all temperatures. Moreover, the results associated with the 10% showed very similar behavior. As the % capture increased, the linear trend was more prominent at lower temperatures versus higher temperatures. This fact was attributed to the larger number of treatment units needed, for the higher capture cases, when compared to the lower capture cases. Figure 4 illustrates the total network cost variation as a function of solvent temperature, for the different CO_2 net capture targets studied. It is evident that the comparison to be made for the entire network cost is completely different than the comparison made when only the treatment cost portion was considered. As shown in Fig. 4, even though an increasing cost trend with respect to solvent temperature was also obtained (as in Fig. 3), there were great differences noted between the various net capture cases. This is because the total network cost accounts for additional cost entities as the piping required by the network, in addition to any pumping and compression costs needed. Moreover, any revenue made by sending treated CO_2 streams into the various sinks, is also considered as part of the total network cost (as a negative entity, indicating revenue made). This is why the 5% and 10% capture cases were more costly when compared to the 20% and 25% capture cases. Moreover, the 45% capture case was far costlier than all the cases

Table 5 Summary of treatment model parameters

Constants for Eq. (6) for MDEA from DiGuilio et al. (1992)	a_1	a_2	a_3	
	1207	− 0.43265	− 0.00047744	
Constants for Eq. (8) for MDEA from DiGuilio et al. (1992)	b_1	b_2	b_3	
	− 4.3039	1266.2	151.4	
Constants for Eq. (20) for MDEA obtained from (Liu et al. 1999)	d_1	d_2	d_3	d_3
	2.01874	− 2.83179	4.11932	− 0.81256
Constants for Eq. (21) for MDEA obtained from (Liu et al. 1999)	e_1	e_2	e_3	e_3
	3135.49	1846.22	2612.63	508.592
Constants for Eq. (22) for MDEA obtained from (Liu et al. 1999)	f_1	f_2	f_3	f_3
	− 813,702	295,623	414,660	− 79,674.6

Fig. 3 Treatment Cost Variation as a Function of solvent temperature, for different CO_2 net capture targets
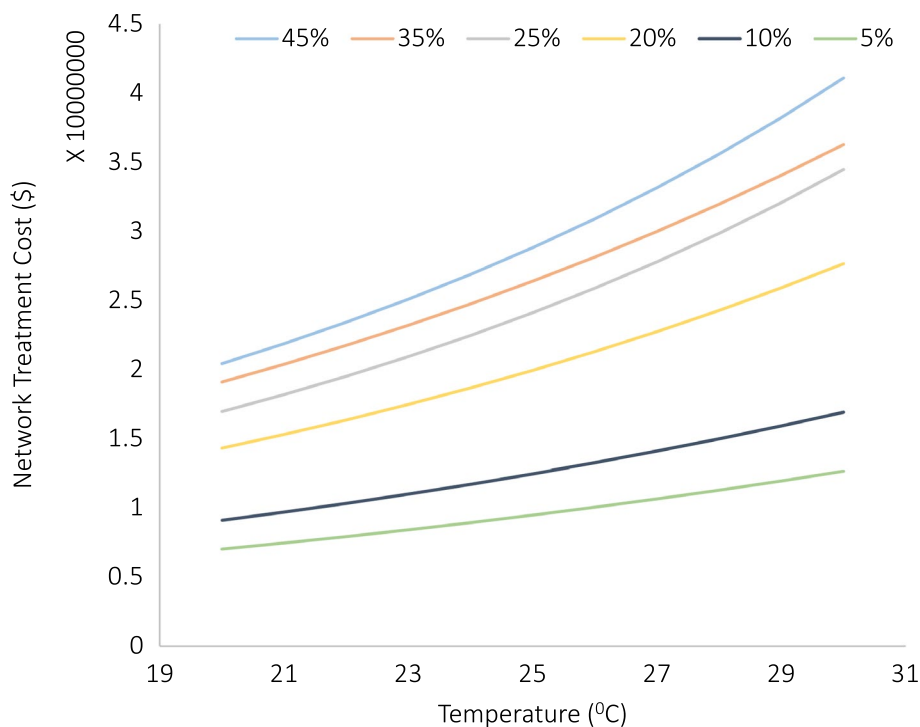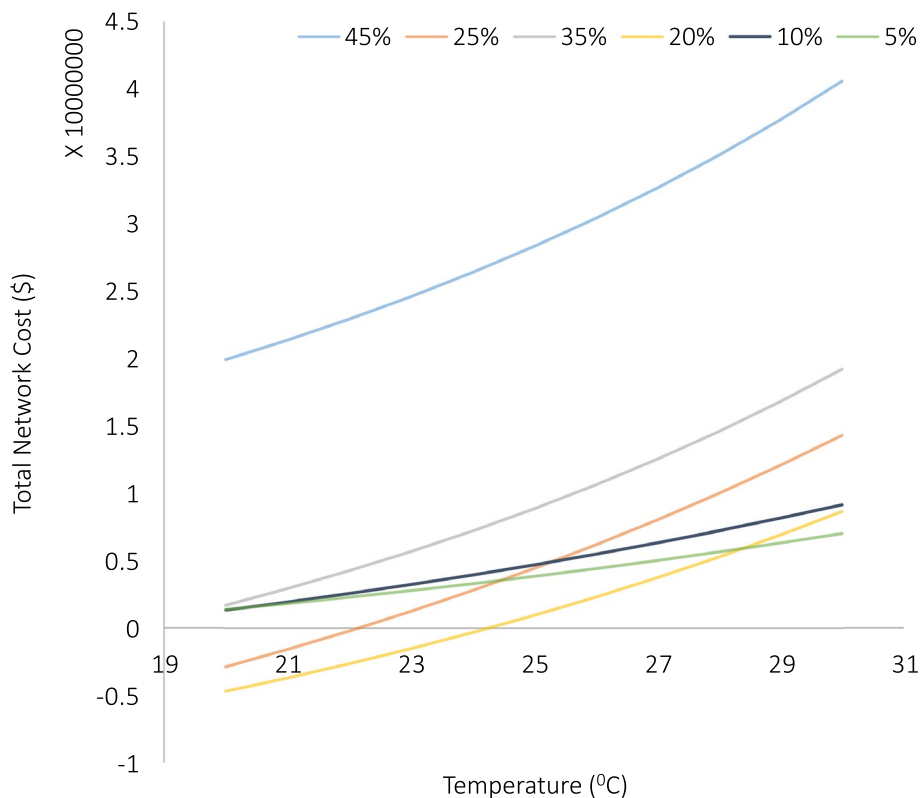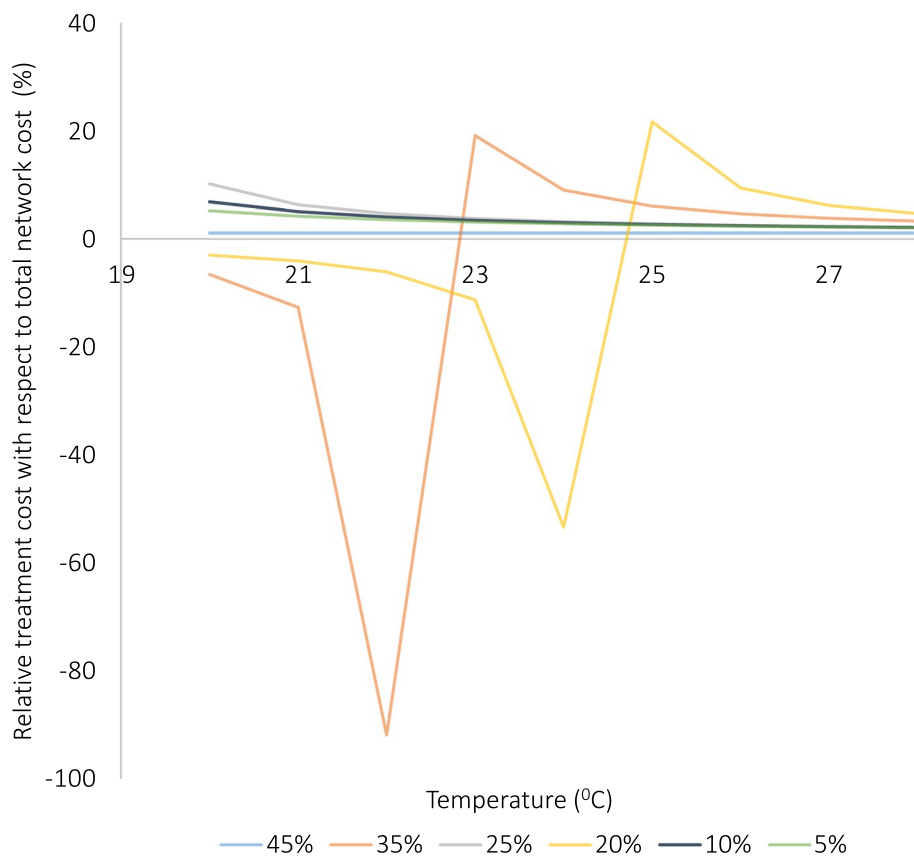

Fig. 4 Total Network Cost Variation as a Function of solvent temperature, for different CO_2 net capture targets

that have been investigated, since the revenue attained from CO_2 sinks was not enough to cover the extra costs needed for treatment and the remaining aspects of the network, unlike the 20% and 25% capture cases. It was also found that the cases that utilized higher solvent temperatures cost more than the lower temperature cases. Hence, it was found that

Fig. 5 Relative Treatment Cost Variation with respect to Total Network Cost, as a Function of solvent temperature, for different CO_2 net capture targets

both the 20% and 25% capture cases were unable to generate any revenue beyond the 25 ^{0}C solvent temperature. In order, be able to compare both, Fig. 5 illustrates the relative treatment cost variation with respect to total network cost, as a function of solvent temperature, for different CO_2 net capture targets. In this figure, it was found that the 25% and the 35% capture cases were the most variant, unlike the remainder of the cases (5%, 10%, 20% and 45%) which simply yielded a decreasing straight line. This indicates that the treatment cost with respect to the total network cost attained for the 25% and 35% cases were very sensitive to the profits attained from the sinks. Initially, at lower temperatures the profit made was much higher compared to the higher temperature cases. For instance, it was found that the profit attained at the CO_2 sinks in the 25% net capture case decreased at 25 °C, compared to the total cost (since the relative treatment cost was no longer negative), while the profit attained by the 25% net capture case decreased at 23 °C. On the other hand, the 5%, 15%, 20% and 45% cases were not able to generate enough revenue at the sinks to yield any net savings. Hence, as the temperature increased, the relative cost remained relatively constant, indicating that the increase in the total cost of the network was proportional to the treatment cost (being the highest cost entity). Moreover, the lower temperature cost cases gave the highest relative cost changes, since the remaining network cost entities were

found to be more significant at the lowest solvent temperature cases (20 °C). Figure 6 further supports this observation, since it shows the relative cost variation of all network cost entities (minus the treatment) which mainly includes piping, compression and pumping, with respect to the Total Network Cost, as a function of solvent temperature, for the different CO_2 net capture targets studied. It should be noted that the same cost breakdown within the carbon integration network was obtained, when comparing the results with the work by (Al-Mohannadi and Linke 2016), with treatment being the highest cost contributor.

When it comes to further investigating the effect varying the solvent temperature on the treatment design attained, Fig. 7 provides some insight into those aspects, as it summarizes the combined change in all column heights that were attained within the CCUS network, with respect to the lowest temperature (20 °C), across all the different net capture targets that have been investigated. According to Fig. 7, the relative combined treatment column heights attained within the network may increase by up to 90% at higher temperatures compared to the design at 20 ^{0}C. On the other hand, the combined treatment column heights attained at lower temperatures were all less than 50% for the cases involving a solvent temperature of less than 25^{0}C. When observing those changes with respect to the lowest net capture case, as opposed to the lowest solvent temperature case, Fig. 8

Fig. 6 Relative Cost Variation of piping, compression and pumping, with respect to the Total Network Cost, as a Function of solvent temperature, for different CO_2 net capture targets
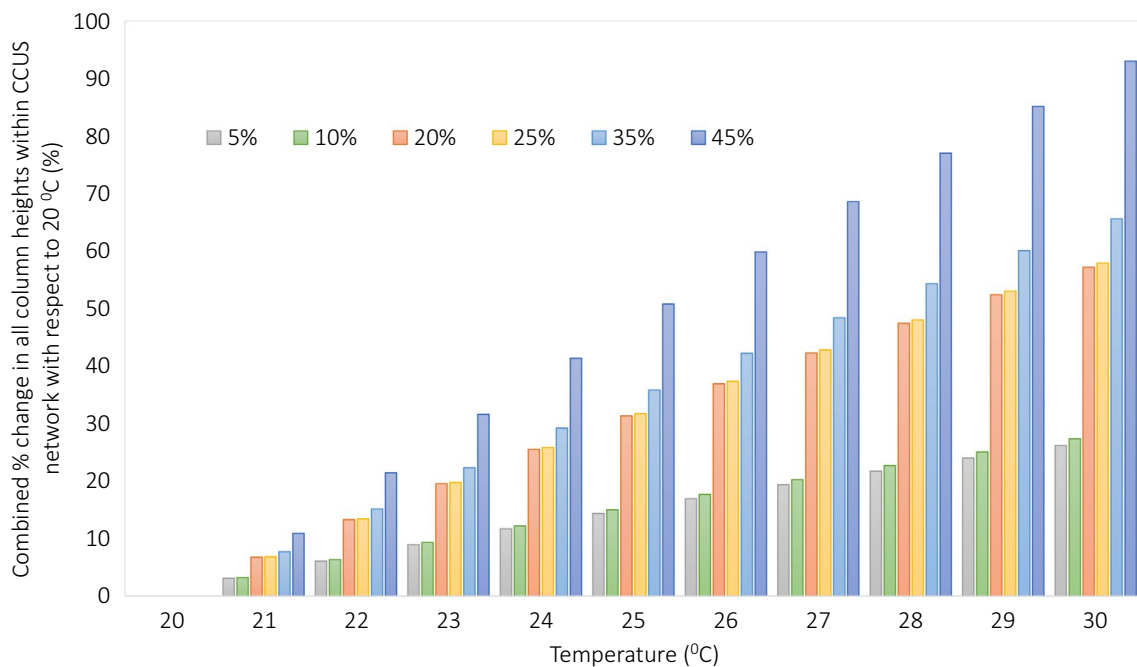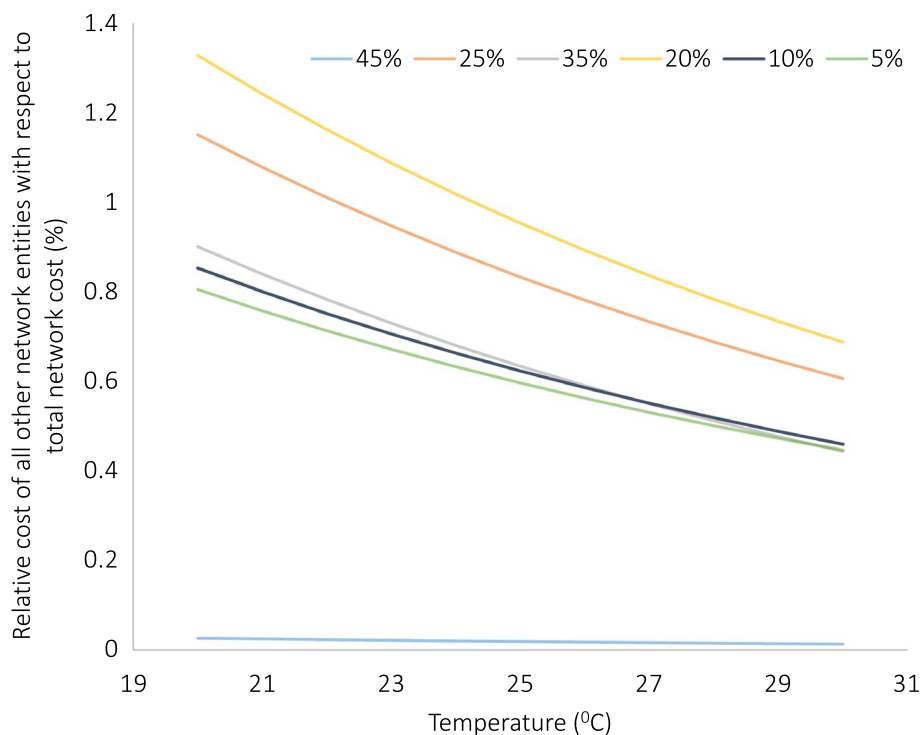
Fig. 7 Column height change attained across all columns within CCUS network for each CO_2 net capture target case, with respect to 20^0C, as a function of the solvent temperature

summarizes those results. For instance, the relative combined treatment column heights attained within the network increased up to 70% at higher temperatures, when compared to the design at 20 °C for the highest capture case. On the other hand, those changes were far less prominent for the 10% capture case, across all temperatures, since the % change varied between around 10%–25%. The three remaining capture cases (20%, 25% and 35%) did not change much
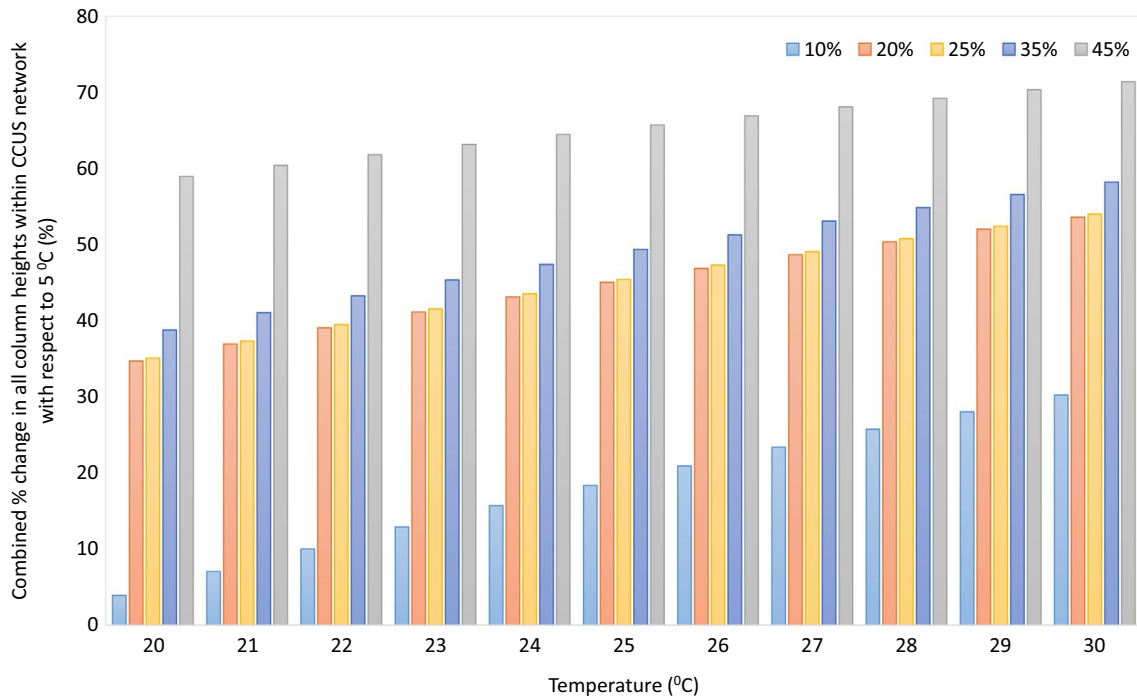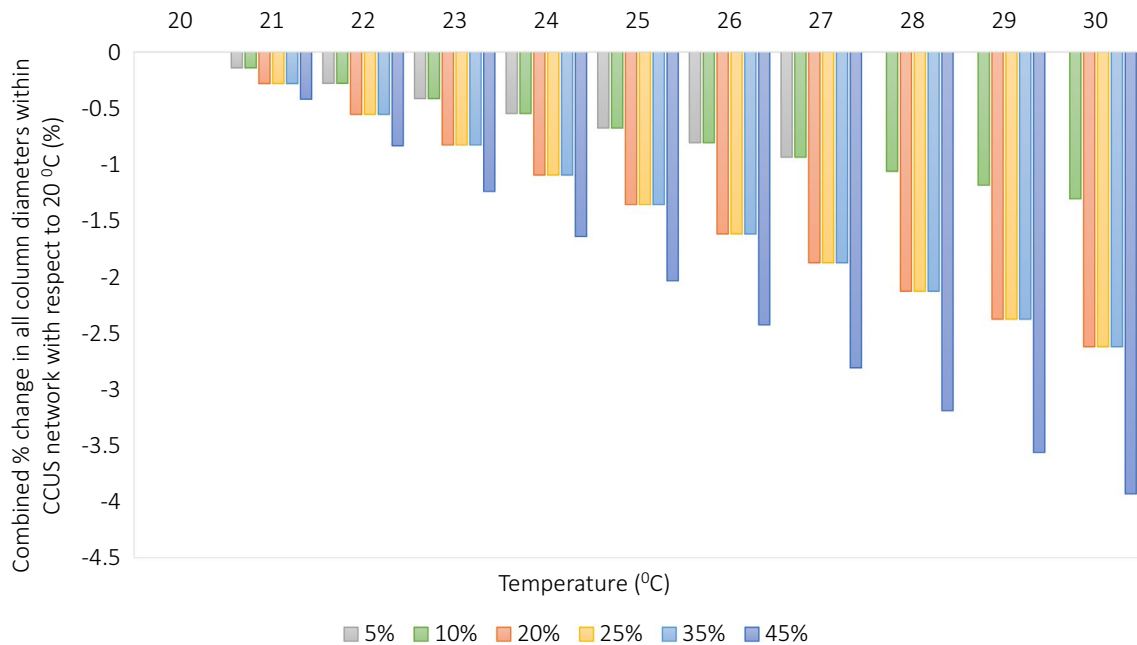
Fig. 8 Column height change attained across all columns within CCUS network tested across the entire temperature range, with respect to the 5% CO_2 net capture target case, as a function of the solvent temperature

in terms of the total column heights across the network, indicating that a similar portfolio of treatment options have been selected across those cases, and those changes were found

to be very minor (when compared to the 5% capture case) at different solvent temperatures, as opposed to the 10% and 45% cases.

Fig. 9 Column diameter change attained across all columns within CCUS network tested across the entire temperature range, with respect to the 20% CO_2 net capture target case, as a function of the solvent temperature

Figure 9 illustrates the combined change in all column diameters that were attained within the CCUS network, with respect to the lowest temperature (20 °C), across all the different net capture targets that have been investigated. According to Fig. 8, the relative combined treatment column diameters exhibited a decreasing trend with increasing solvent temperatures, when compared to the design at 20 °C, unlike the combined column heights. Nonetheless, those changes were still quite minor. When observing the combined column diameter changes attained with respect to the lowest net capture case for all the CCUS networks that were studied, as opposed to the lowest solvent temperature case, Fig. 10 summarizes those results. For instance, the relative combined treatment column diameters attained within the network increased up to 75% at higher temperatures, when compared to the design at 20 °C for the highest capture case. A very similar trend was observed for combined column heights in Fig. 8, for the highest capture case. On the other hand, the diameter changes were far more prominent for the 10% capture case, across all temperatures, since the % change varied reached up to 40%, unlike the 10%–25% changes observed in the column height. This indicated the column diameter sensitivity to changes in solvent temperature, for the low net capture target cases. The three remaining capture cases (20%, 25% and 35%) did not change much in terms of the total column diameters across the network, just like the column height, indicating that a similar portfolio of treatment options have been selected across those cases, and those changes were also found to be very minor (when compared to the 5% capture case) for different solvent temperatures, as opposed to the 10% and 45% cases.

Conclusions

This paper studies the effect of incorporating a modified treatment model on the overall performance of CO_2 network under different CO_2 net capture targets. The treatment model utilizes all the necessary treatment design parameters to be assessed within the network has been integrated to the original network problem formulation, which has been presented previously by Al-Mohannadi and Linke (2016). Unlike the original model, in which many of the cost items have been lumped into single parameters in the original formulation, this work expands the treatment stage calculations in order to accommodate more variables and As it has been demonstrated in this paper, utilizing a more detailed cost model was found to be very helpful in understanding the effect of solvent temperature on the overall performance of carbon integration systems, especially when subjected to varying the net emission reduction targets. In order to illustrate the modified model, a total of 6 capture cases have been investigated in this work, by varying the solvent temperature between 20 °C and 30 °C. All the results which have been obtained have been discussed and summarized, and much insight has been provided in terms of the effects observed, onto the overall network cost and performance attained. An increase in the total cost of the network was observed as the solvent operating temperature in the treatment unit was
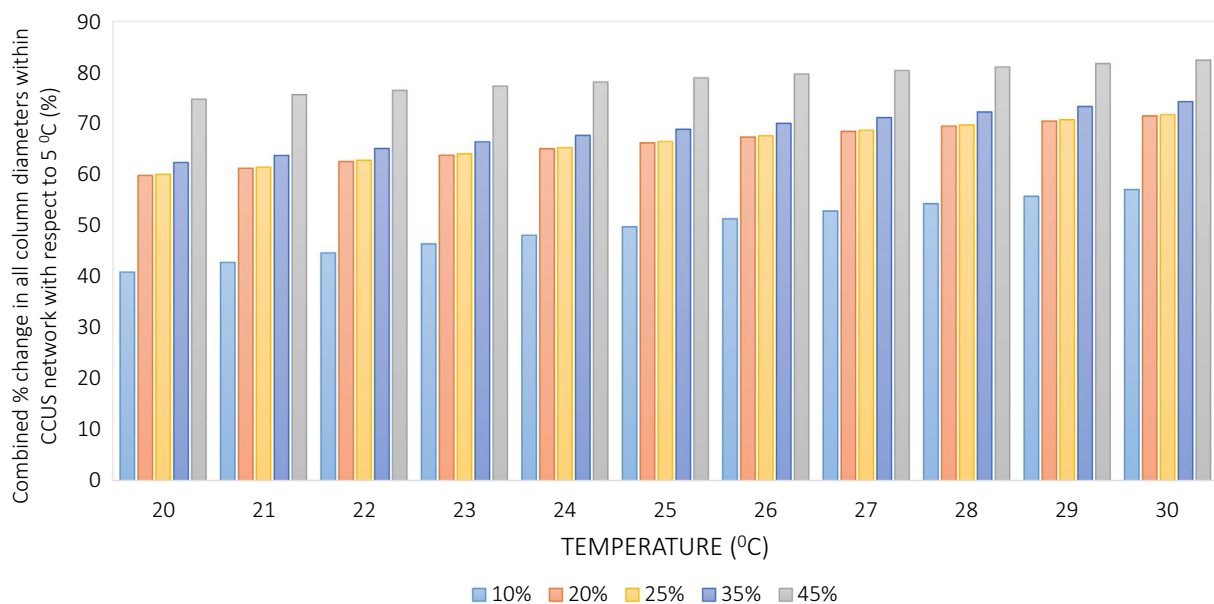

Fig. 10 Column diameter change attained across all columns within CCUS network tested across the entire temperature range, with respect to the 5% CO_2 net capture target case, as a function of the solvent temperature

increased. However, as the total net CO_2 captured increased, a linear trend was more prominent at lower temperatures versus higher temperatures, which in turn exhibited a non-linear increase. Additionally, it was found that at 20% and 25% net capture targets, no sink revenue can be generated beyond the 25 °C solvent temperatures. Moreover, the optimal treatment column diameter was more sensitive to changes in solvent temperatures for the low net capture target cases (below 10%), and was less sensitive to solvent temperature changes at higher capture targets (above 10%). In future research, it is recommended to explore different types of carbon capture technologies, including membrane treatment, precapture technologies, and carbonate capture. Investigating these alternative approaches will contribute to establishing a deeper understanding and certainly help identify further potential improvements in carbon capture methods.

Author contributions S.A. Concept, Method and Writing. D.M. Concept, Writing and Review.

Declarations

Competing interests The authors declare no competing interests.

References

Al-Mamoori A, Krishnamurthy A, Rownaghi AA, Rezaei F (2017) Carbon capture and utilization update. Energy Technol 5(6):834–849

Al-Mohannadi DM, Linke P (2016) On the systematic carbon integration of industrial parks for climate footprint reduction. J Clean Prod 112:4053–4064

Al-Mohannadi DM, Linke P, Bishnu SK, Alnouri SY (2015) Interplant carbon integration towards phased footprint reduction target. In: Gernaey KV, Huusom JK, Gani R (eds) Computer aided chemical engineering, vol 37. Elsevier, Amsterdam, pp 2057–2062

Brunazzi E, Festa UD, Galletti C, Merello C, Paglianti A, Pintus S (2002) Measuring volumetric phase fractions in a gas–solid–liquid stirred tank reactor using an impedance probe. Can J Chem Eng 80(4):1–7

Budinis S, Krevor S, Dowell NM, Brandon N, Hawkes A (2018) An assessment of CCS costs, barriers and potential. Energ Strat Rev 22:61–81

Centi G, Perathoner S (2023) The chemical engineering aspects of CO2 capture, combined with its utilisation. Curr Opin Chem Eng 39:100879

de Meyer F, Bignaud C (2022) The use of catalysis for faster CO_2 absorption and energy-efficient solvent regeneration: an industry-focused critical review. Chem Eng J 428:131264

DiGuilio RM, Lee RJ, Schaeffer ST, Brasher LL, Teja AS (1992) Densities and viscosities of the ethanolamines. J Chem Eng Data 37(2):239–242

Fagorite VI, Onyekuru SO, Opara AI, Oguzie EE (2023) The major techniques, advantages, and pitfalls of various methods used in geological carbon sequestration. Int J Environ Sci Technol 20(4):4585–4614

Goldthorpe S (2017) Potential for very deep ocean storage of CO_2 without ocean acidification: a discussion paper. Energy Procedia 114:5417–5429

Gonzalez K, Boyer L, Almoucachar D, Poulain B, Cloarec E, Magnon C, de Meyer F (2023) CO_2 and H_2S absorption in aqueous MDEA with ethylene glycol: electrolyte NRTL, rate-based process model and pilot plant experimental validation. Chem Eng J 451:138948

Guduru RK, Gupta AA, Dixit U (2022) Chapter 13 - Biological processes for CO_2 capture. In: Khalid M, Dharaskar SA, Sillanpää M, Siddiqui H (eds) Emerging carbon capture technologies. Elsevier, Amsterdam, pp 371–400

Hospital-Benito D, Lemus J, Moya C, Santiago R, Ferro VR, Palomar J (2021) Techno-economic feasibility of ionic liquids-based CO2 chemical capture processes. Chem Eng J 407:127196

Hussin F, Aroua MK (2020) Recent trends in the development of adsorption technologies for carbon dioxide capture: A brief literature and patent reviews (2014–2018). J Clean Prod 253:119707

IEA (2019). World Energy Outlook Paris.

IPCC (2005). IPCC special report on carbon dioxide capture and storage. In: Metz B, Davidson O, Coninck HCD, Loos M, Meyer LA (eds). Cambridge

Li K, Leigh W, Feron P, Yu H, Tade M (2016) Systematic study of aqueous monoethanolamine (MEA)-based CO_2 capture process: techno-economic assessment of the MEA process and its improvements. Appl Energy 165:648–659

LINDO®. (2023) Software for integer programming, linear programming, nonlinear programming, stochastic programming, Global Optimization." Retrieved May, 2023, from https://www.lindo.com/.

Liu H-B, Zhang C-F, Xu G-W (1999) A study on equilibrium solubility for carbon dioxide in Methyldiethanolamine−Piperazine−Water solution. Ind Eng Chem Res 38(10):4032–4036

Luis P (2016) Use of monoethanolamine (MEA) for CO_2 capture in a global scenario: consequences and alternatives. Desalination 380:93–99

Madejski P, Chmiel K, Subramanian N, Kuś T (2022) "Methods and Techniques for CO2 Capture: Review of Potential Solutions and Applications in Modern Energy Technologies. Energies 1:5. https://doi.org/10.3390/en15030887

Najjar YSH (2008) Modern and appropriate technologies for the reduction of gaseous pollutants and their effects on the environment. Clean Technol Environ Policy 10(3):269–278

Ochedi ET, Taki A (2022) A framework approach to the design of energy efficient residential buildings in Nigeria. Energy Built Environ 3(3):384–397

Xu A, Indala S, Hertwig TA, Pike RW, Knopf FC, Yaws CL, Hopper JR (2005) Development and integration of new processes consuming carbon dioxide in multi-plant chemical production complexes. Clean Technol Environ Policy 7(2):97–115

Zahid U (2020) Simulation of an acid gas removal unit using a DGA and MDEA blend instead of a single amine. Chem Product Process Model 15:4. https://doi.org/10.1515/cppm-2019-0044

Zhang S, Shen Y, Wang L, Chen J, Lu Y (2019) Phase change solvents for post-combustion CO_2 capture: Principle, advances, and challenges. Appl Energy 239:876–897

Zhang Z, Pan S-Y, Li H, Cai J, Olabi AG, Anthony EJ, Manovic V (2020) Recent advances in carbon dioxide utilization. Renew Sustain Energy Rev 125:109799